



*Research article*

## **HB-EGF and ADAM 12S directed cellular reprogramming results in metabolically active brown adipose tissue-like cells**

**Sean R. Taylor, Carly A. Gemma, Kayla M. Cartwright, Daniel C. Pfeil, Evan R. Miller, Charles E. Long and Paul A. Harding\***

Department of Biology, Miami University, Oxford, OH 45056

**\*Correspondence:** Email: [hardinpa@miamioh.edu](mailto:hardinpa@miamioh.edu); Tel: 5137273447.

**Abstract:** Brown adipose tissue (BAT) is considered a potential tool for the treatment of obesity and type 2 diabetes due to its ability to uncouple oxidative phosphorylation and stimulate non-shivering thermogenesis that utilizes glucose and lipids as its source of energy. Previous results from our lab demonstrated that co-expression of HB-EGF and ADAM 12S resulted in lipid accumulation and a BAT-like phenotype, including up-regulation of BAT genes, down-regulation of genes involved in formation of white adipose tissues, and increased mitochondrial staining in three cell lines including mouse fibroblasts, human epidermoid carcinoma cells, and human preadipocytes. Furthermore, qRT-PCR results demonstrated up-regulation of cellular reprogramming factors such as KLF4, KLF3, and FGF-2 and down-regulation of LMNA, a marker gene involved in differentiation, in the BAT-like reprogrammed cells. This study substantiates these findings using immunohistochemical analysis of reprogrammed BAT-like cells that demonstrate increased immunofluorescent detection of FGF-2, KLF3, and PGC-1 $\alpha$  and decreased immunofluorescence for C/EBP $\alpha$ . Supportive evidence of cellular reprogramming involves the use of a stem-cell transcription factor RT-profiler array that results in enhanced expression of HOXA10 (3.04-fold) and HOXC5 (6.46-fold). In order to demonstrate that HB-EGF/ADAM 12S reprogrammed BAT-like cells function as BAT, oxygen consumption and extracellular acidification rates were measured using a Seahorse XFe24 Analyzer with and without catecholamine exposure followed by FCCP + Oligomycin exposure. HB-EGF/ADAM 12S reprogrammed BAT-like cells demonstrate a significant metabolic increase compared to MLC, HB-EGF, ADAM 12S. HB-EGF/ADAM12S reprogrammed BAT-like cells exhibit a metabolic profile similar to 3T3-L1 induced BAT cells. Collectively, these results demonstrate that HB-EGF/ADAM 12S co-expression stimulates cellular reprogramming into metabolically active BAT and may be a putative therapeutic tool to combat obesity and type 2 diabetes.

**Keywords:** cellular reprogramming; brown adipose tissue; HB-EGF; ADAM 12S; obesity

---

## 1. Introduction

Adipose tissue (AT) is an important tissue for maintaining homeostasis by providing protection, energy storage, and heat generation that likely evolved as adaptations to limited food supplies and temperature fluctuations [1,2]. While white AT (WAT) provides protection and energy storage [3], brown AT (BAT) is responsible for heat production during times of cold stress by non-shivering thermogenesis [4]. BAT is characterized by abundant mitochondria that express uncoupling protein 1 (UCP-1) which dissipates energy as heat when exposed to cold or to adrenergic stimulation resulting in the uncoupling of oxidative phosphorylation from ATP synthesis [5]. Interestingly, some WAT has the ability to express UCP-1 when exposed to  $\beta_3$ -adrenergic receptor agonists or in response to cold acclimation and are often referred to as beige or brite cells [6]. It is hypothesized that increasing the mass of either BAT or beige cells is likely to result in reduction of body weight, fat mass, improved insulin sensitivity and glucose metabolism. Therefore, the ability to reprogram WAT into BAT is likely a logical therapeutic approach to combat obesity and type 2 diabetes [1]. Recently our lab has reported that mouse fibroblasts (MLC) and human epidermoid carcinoma (A431) cells can be reprogrammed into BAT-like cells when co-expressing HB-EGF and ADAM12S [7,8]. These cells demonstrated increased mRNA expression of the BAT marker gene PGC-1 $\alpha$  and reprogramming factors fibroblast growth factor (FGF)-2, Kruppel Like Factor (KLF) 3 and 4. Additionally these cells demonstrated down-regulation of the WAT marker gene CCAAT/Enhancer Binding Protein (C/EBP $\alpha$ ) and lamin A/C (LMNA) which is needed to maintain the somatic state of cells.

The remodeling of the extracellular matrix (ECM) is important for determining adipocyte phenotype [1,9,10]. Proteolytic processing of heparin-binding epidermal growth factor-like growth factor (HB-EGF) may play a role in this remodeling. HB-EGF is a type I transmembrane protein that undergoes substantial post-translational modification. The endoprotease furin initially processes the extracellular domain at Arg62-Asp63 [11], cleaving the 208 amino acid proHB-EGF precursor which can be further processed by a disintegrin and metalloprotease (ADAM) between Pro148-Val149 or Glu151-ASN152 resulting in the release of mature HB-EGF into the extracellular environment, termed ectodomain shedding [12]. Upon ectodomain shedding of proHB-EGF by ADAMs, further intracellular processing by an unidentified protease results in a carboxy terminal fragment (HB-EGF C) that migrates to the nucleus and alleviates a transcriptional repressor promyelocytic leukemia zinc finger (PLZF) and results in increased cellular division [13]. One protease, ADAM12, has been reported to cleave membrane bound HB-EGF in the N-terminus thus releasing soluble (s) HB-EGF [14]. The ADAM family of transmembrane metalloprotease-disintegrins encodes a very unique domain organization including a signal peptide, pro-, metalloprotease (zinc binding site), disintegrin, cysteine-rich, transmembrane, and cytoplasmic domains. ADAM12 can be found in both a membrane bound form (ADAM12L) and a secreted form (ADAM12S) as a result of alternative splicing. ADAM 12S has been associated with a number of physiological activities including extracellular-matrix remodeling, myogenesis, and adipogenesis [15,16].

Mature, soluble HB-EGF and HB-EGF C each exhibit mitogenic activity and thus are stimulators of cellular proliferation in an EGFR-dependent and EGFR-independent manner, respectively [17].

However, recent evidence from our lab suggests HB-EGF/ADAM12S co-expressing cells attenuates cellular proliferation and promotes lipid accumulation [7]. Additionally, HB-EGF/ADAM12S co-expressing cells exhibit increased immunofluorescence for FGF-2, KLF3, and PGC-1 $\alpha$  and decreased immunofluorescence for C/EBP $\alpha$  and GLUT4 as well as increased HOXA10 and HOXC5 expression. Assessment of the metabolic activity of HB-EGF/ADAM12S reprogrammed cells closely reflect the metabolic activity of BAT. Collectively, this report provides evidence for a novel cellular reprogramming pathway that is not yet completely understood, yet is dependent at least upon processing of HB-EGF by ADAM 12S.

## 2. Materials and methods

### 2.1. Generation of stable mammalian cell lines

Mouse fibroblasts (MLCs, ATCC# CRL-2648) were maintained in Dulbecco's Modified Eagle Medium (DMEM, Cellgro, Herndon, VA) which was supplemented with 10% fetal bovine serum, and penicillin/streptomycin (100  $\mu$ g/mL each) (BioWhittaker, Walkersville, MD). Cells reached approximately 70% confluence and were transfected with, Mock, HB-EGF or ADAM12S with Viafect transfection reagent (Promega, Madison, WI) according to manufacturer's recommendations. Forty-eight hours post transfection, cells were placed on G418 selection (1.0 mg/mL, Invitrogen, Carlsbad, CA) or Blasticidin (10.0  $\mu$ g / mL, Invitrogen). Once selection had occurred HB-EGF cells were further transfected with ADAM12S in the same manner. Co-transfected cells were placed on dual selection of G418 and Blasticidin (10.0  $\mu$ g/mL).

### 2.2. Immunohistochemical analysis of proteins

Mouse fibroblasts (MLCs) and MLCs co-expressing HB-EGF/ADAM 12S were seeded at 70,000 cells per well in 48 well plates and grown to approximately 70% confluence. They were fixed with 4% paraformaldehyde. Cells were then permeabilized with phosphate buffered saline containing 1% Triton-X-100 (PBST) for 10 minutes at room temperature. The cells were then incubated with either no primary antibody, or primary antibodies rabbit anti-FGF2 peptide antibody (Sigma-Aldrich, St. Louis, MO), rabbit anti-KLF3 peptide antibody (Sigma-Aldrich, St. Louis, MO), affinity isolated goat anti-PGC-1 $\alpha$  antibody (Sigma-Aldrich, St. Louis, MO), rabbit anti-C/EBP- $\alpha$  peptide antibody (Sigma-Aldrich, St. Louis, MO), and rabbit anti-GLUT4 affinity isolated antibody (Sigma-Aldrich, St. Louis, MO). Cells were washed 3 times with PBS, 5 minutes each, then incubated with secondary antibody, conjugated goat anti rabbit -fluorescein (FITC) (Jackson, West Grove, PA) in 0.1M PBS. The cells were stained with DAPI, imaged, and quantitated by counting the number of fluorescent cells using a fluorescent microscope (Olympus).

### 2.3. Stem-cell transcription factor RT2 profiler array

Total cellular RNA was isolated from tissue culture plates of A431 MOCK transfected cells and A431 cells co-expressing HB-EGF/ADAM 12S using RNeasy Lipid Tissue Mini Kit from Qiagen making use of TRIzol lysis agent. 3.932  $\mu$ g of RNA for each sample was reverse transcribed using RT2 First Strand Kit from Qiagen, which includes DNase treatment in the genomic elimination

mixture. The cDNA was generated for A431 Mock cells and HB-EGF/ADAM 12S stable cells and combined with RT2 SYBR Green Fluor qPCR Master Mix and carried out in triplicate using the Human Stem-cell Transcription Factor RT2 Profiler Array (Qiagen). All procedures were carried out according to manufacturer's protocol. 25  $\mu$ L of the cDNA SYBR Green mixture were loaded in each well of a 96 well plate containing primers for 84 genes of interest. Biorad CFX connect was used for PCR, 1 cycle 95°C for 10 minutes, 40 cycles 95°C for 15 seconds and 60°C for 60 seconds and data analysis was performed using Qiagen's online data analysis software (<http://pcrdataanalysis.sabiosciences.com/pcr/arrayanalysis.php>) using the  $\Delta\Delta$ Ct method. Fold changes were calculated for each gene using the difference between RNA from cells co-expressing HB-EGF/ADAM 12S and control RNA where a positive value represents up-regulation in HB-EGF/ADAM 12S co-expressing cells and a negative value represents down-regulation.

#### 2.4. Induction of BAT and WAT from 3T3-L1 cells

3T3-L1 (ATCC® CL-173™) cells were cultured and maintained in growth medium (DMEM supplemented with 10% fetal bovine serum and penicillin/streptomycin (100  $\mu$ g/mL each)). Cells reached 70% confluence and then were differentiated using WAT differentiation media (Dex (0.25  $\mu$ M), IBMX (0.5 mM) and Ins (10  $\mu$ g/mL)) for 2 days, or BAT differentiation media (Dex (0.25  $\mu$ M), IBMX (0.5 mM), Ins (10  $\mu$ g/mL), Rosiglitazone (1  $\mu$ M), T3 (50 nM)) for 2 days, followed by culture in growth medium supplemented with Ins (5  $\mu$ g/mL) as previously demonstrated [18]. On day eight, lipid accumulation was examined and samples were prepared for oxygen consumption and extracellular acidification rate experiments on the Seahorse instrument.

#### 2.5. Metabolic activity

Metabolic data was tested for and results were collected based on manufacturer's recommended protocol. Cells were plated at a density of 30,000 cells per well in Seahorse XF24 assay plates (Seahorse Bioscience, Chicopee, MA) and the sensor cartridge was hydrated overnight at 37°C in a non-CO<sub>2</sub> incubator the day before the assay. The day of the assay, Seahorse XF Base Medium was supplemented with 1mM pyruvate, 2mM Glutamax, and 10mM glucose and pHed to 7.4 with 0.1N NaOH at 37°C. Cell growth media was then removed after confirming desired cell confluence; washed cells with warmed assay medium and added 500 $\mu$ L of assay medium to each well. Seahorse XF Cell Energy Phenotype Test Kit (Seahorse Bioscience) was employed to observe metabolic rate. FCCP (100  $\mu$ M) and Oligomycin (100  $\mu$ M) stock solutions were prepared and then the stressor mix was made with 2400  $\mu$ L of Assay medium, and 300  $\mu$ L of Oligomycin and FCCP stock solutions each. Catecholamines (Dionex,) stock solution (1 mg/mL dopamine, norepinephrine, epinephrine) was made into a working solution [4  $\mu$ g/mL] and insulin working solution was made at [5  $\mu$ g/mL]. The assay was run according to manufacturer's recommendations for 4 cycles of 3 loops each time; first basal, second catecholamines, then insulin, and finally the stressor mix. Each loop injected the drug of choice: Catecholamines (50  $\mu$ L), Insulin (100  $\mu$ L), and stressor mix (56  $\mu$ L), before shaking for 1 minute and then probing for 3 minutes. Insulin and catecholamine treatment of HB-EGF/ADAM 12S expressing cells. Results were then analyzed using a student's t-test and standard error of the mean reported.

### 3. Results

### 3.1. Immunofluorescence of proteins

In order to substantiate previous results in mRNA expression due to HB-EGF/ADAM 12S co-expression, immunohistochemistry (IHC) was performed to detect expression of FGF2, KLF3, PGC-1 $\alpha$ , C/EBP- $\alpha$ , and GLUT4 protein levels. HB-EGF/ADAM 12S co-expressing cells demonstrate increased immunofluorescence of FGF2 by  $\sim$ 1.2 fold (Figure 1 panels A,C,E) ( $n = 4$ ), KLF3 by  $\sim$ 1.5 fold (Figure 2 panels A,C,E) ( $n = 4$ ), no significant change in PGC-1 $\alpha$  (Figure 3 panels A,C,E) ( $n = 4$ ), and decreased immunofluorescence of C/EBP- $\alpha$  by  $\sim$ 2 fold (Figure 4 panels A,C,E) ( $n = 4$ ), and GLUT4 by  $\sim$ 1.3 fold (Figure 5 panels A,C,E) ( $n = 4$ ). Interestingly, expression of FGF2, PGC-1 $\alpha$ , and Glut4 appear to be localized throughout the co-transfected cells and mostly localized in the nucleus of control cells. These findings reflect the results from the previously reported mRNA expression [8].

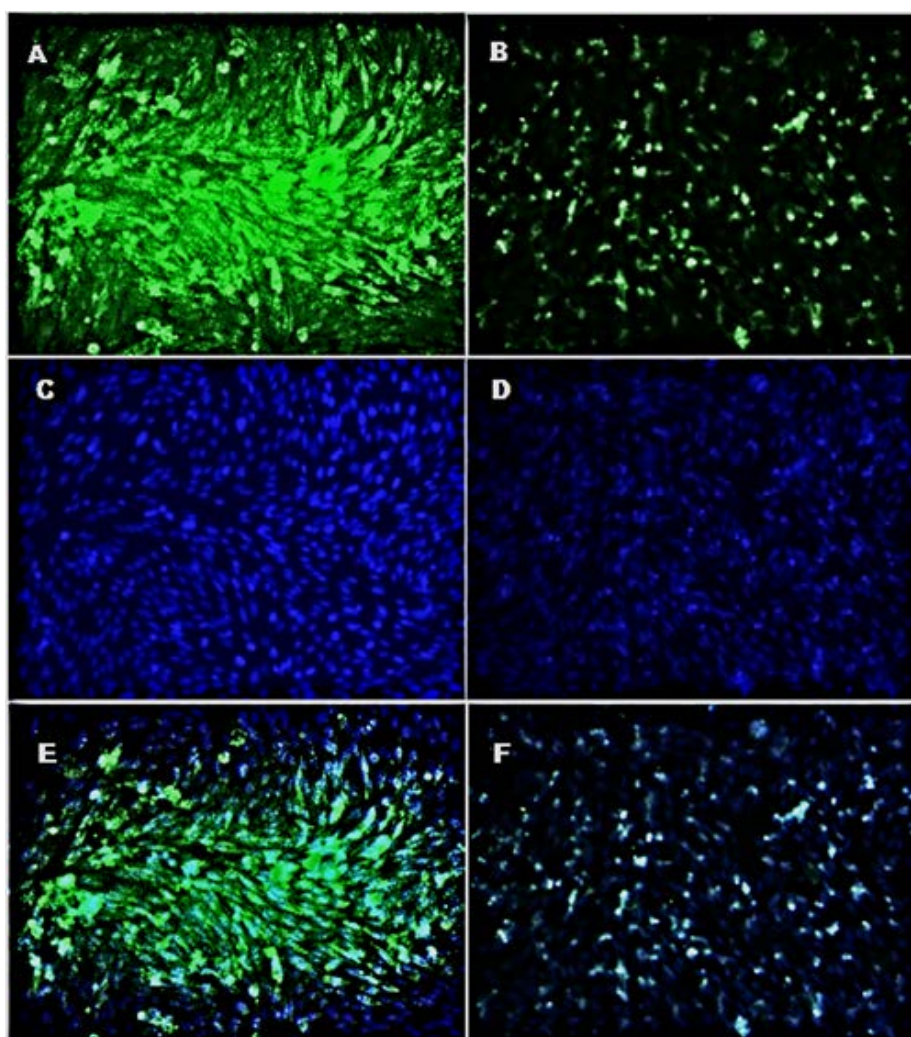


**Figure 1.** Immunohistochemical analysis of FGF2 in HB-EGF/ADAM 12S co-expressing cells. Cells were fixed, FGF2 primary antibody was added, washed and then probed with FITC secondary antibody (A,B). The nucleus was then stained with DAPI (C,D) and images were merged (E,F) to determine expression. Images were taken using the 20x objective lens (Olympus). HB-EGF/ADAM 12S co-expressing cells (A,C,E) demonstrate increased immunofluorescence for FGF2 compared to controls (B,D,F). Images are representative of 4 individual stainings.

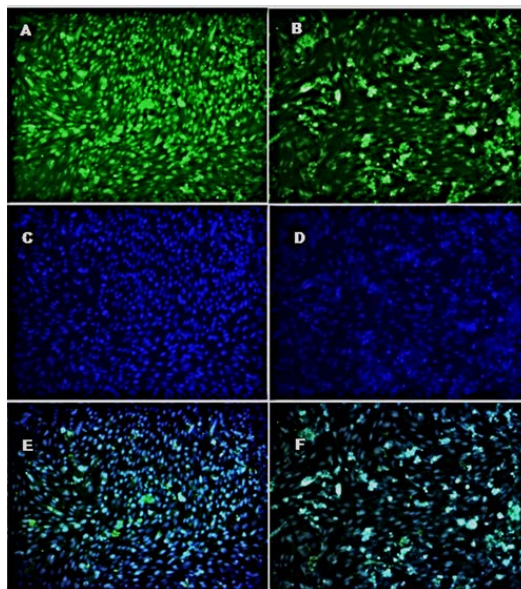


**Figure 2.** Immunohistochemical analysis of KLF3 in HB-EGF/ADAM 12S co-expressing cells. Cells were fixed, KLF3 primary antibody was added, washed, and then probed with FITC secondary antibody (A,B). The nucleus was then stained with DAPI (C,D) and images were merged (E,F) to determine expression. Images were taken using the 20 $\times$  objective lens (Olympus). HB-EGF/ADAM 12S co-expressing cells (A,C,E) demonstrate increased immunofluorescence for KLF3 compared to controls (B,D,F). Images are representative of 4 individual stainings.

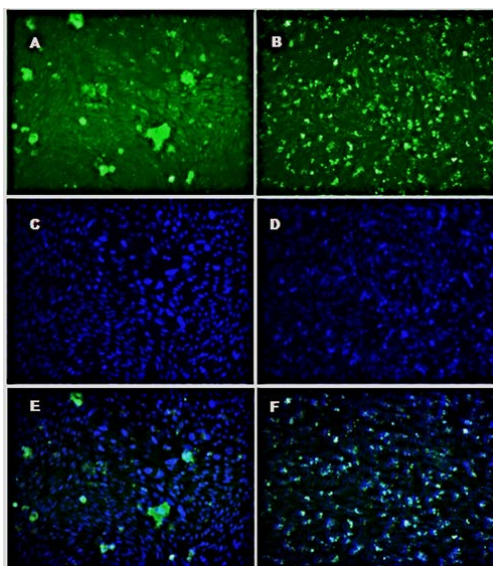


**Figure 3.** Immunohistochemical analysis of PGC-1 $\alpha$  in HB-EGF/ADAM 12S co-expressing cells. Cells were fixed, PGC-1 $\alpha$  primary antibody was added, washed, and then probed with FITC secondary antibody (A,B). The nucleus was then stained with DAPI (C,D) and images were merged (E,F) to determine expression. Images were taken using the 20 $\times$  objective lens (Olympus). HB-EGF/ADAM 12S co-expressing cells (A,C,E) demonstrate increased immunofluorescence for PGC-1 $\alpha$  compared to controls (B,D,F). Images are representative of 4 individual stainings.

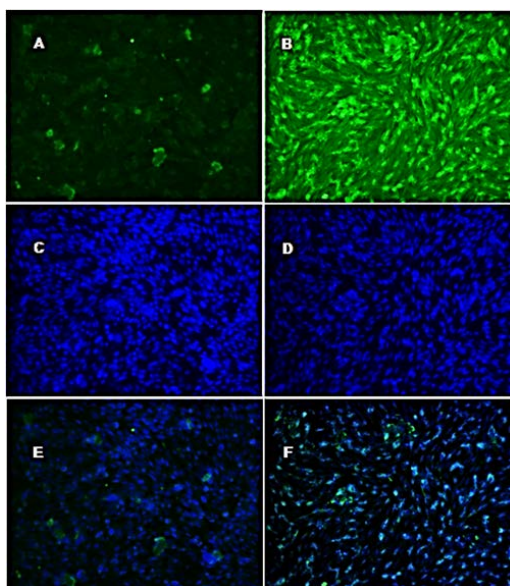


**Figure 4.** Immunohistochemical analysis of C/EBP- $\alpha$  in HB-EGF/ADAM 12S co-expressing cells. Cells were fixed, C/EBP- $\alpha$  primary antibody was added, washed, and then probed with FITC secondary antibody (A,B). The nucleus was then stained with DAPI (C,D) and images were merged (E,F) to determine expression. Images were taken using the 20x objective lens (Olympus). HB-EGF/ADAM 12S co-expressing cells (A,C,E) demonstrate decreased immunofluorescence for C/EBP- $\alpha$  compared to controls (B,D,F). Images are representative of 4 individual stainings.

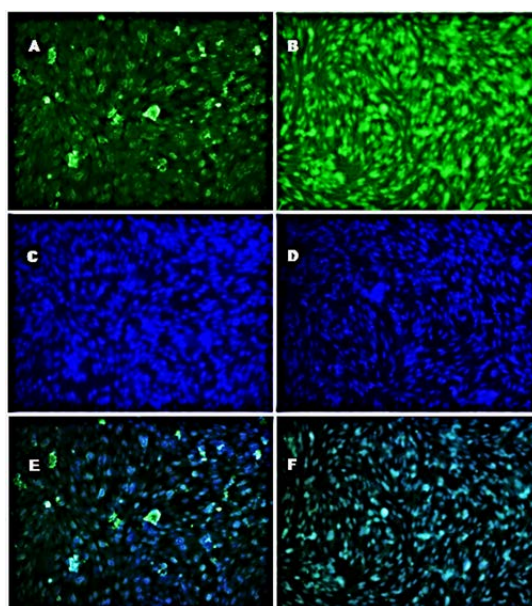


**Figure 5.** Immunohistochemical analysis of GLUT4 in HB-EGF/ADAM 12S co-expressing cells. Cells were fixed, GLUT4 primary antibody was added washed and then probed with FITC secondary antibody (A,B). The nucleus was then stained with DAPI (C,D) and images were merged (E,F) to determine expression. Images were taken using the 20 $\times$  objective lens (Olympus). HB-EGF/ADAM 12S co-expressing cells (A,C,E) demonstrate decreased immunofluorescence for GLUT4 compared to controls (B,D,F). Images are representative of 4 individual stainings.

### 3.2. Stem-cell Transcription Factors

Results from the adipogenic profiler array suggest that HB-EGF/ADAM 12S co-expressing cells may potentially be going through a stem-like cell state prior to be reprogrammed into a BAT-like cell. In order to further investigate these results, a stem-cell transcription factors profiler array was conducted using mock A431 RNA and HB-EGF/ADAM 12S co-expressing RNA in order to assess genes that may be involved in stem cell expression. Results from these studies demonstrated that HOXA10 (3.041) and HOXC5 (6.458) were both up-regulated while HOXA7, HOXC10, and PAX9 were not (Figure 6).

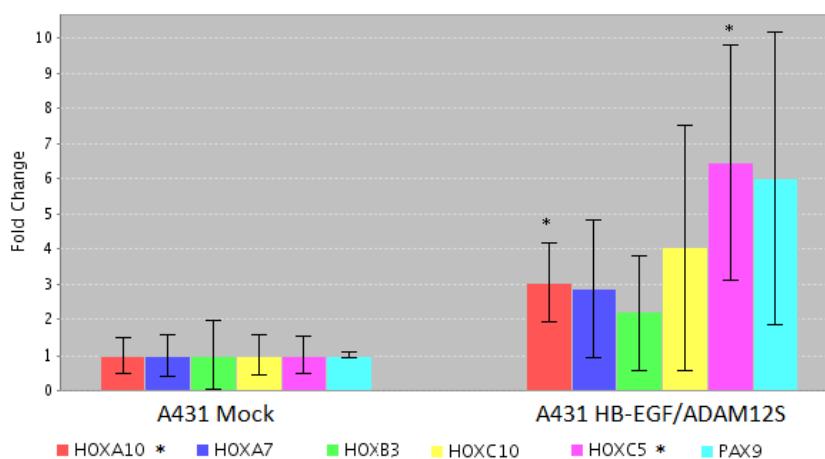


**Figure 6.** Gene expression of stem cell transcription factors in HB-EGF/ADAM 12S co-expressing A431 cells. 96 well qPCR microarrays were used on the Bio-Rad CFX Connect and differential gene regulation was determined (n = 3). HOXC5 and HOXA10 were up-regulated.

### 3.3. Metabolic Output of HB-EGF/ADAM 12S MLCs.

Administration of insulin prior to or after catecholamine exposure on MLC, HB-EGF, ADAM 12S, and HB-EGF/ADAM 12S co-expressing cells had no effect on metabolic activity and are reported together to better provide glycolytic and oxidative phosphorylation activity. When comparing glycolytic profiles (ECAR), basal metabolism was determined for MLC (20.9 mpH/min), HB-EGF (19.2 mpH/min), ADAM12S (17.0 mpH/min), and HB-EGF/ADAM12S (17.05 mpH/min), suggesting no significant difference between the basal metabolic rates of these cell lines. Comparison of each cell types basal rates to catecholamine exposure, only HB-EGF (13.8 mpH/min) was significantly down regulated upon exposure to catecholamines. Basal rates were compared to when exposed to FCCP+Oligomycin in MLC (45.1 mpH/min), HB-EGF (33.1 mpH/min), ADAM12S (32.9 mpH/min) and HB-EGF/ADAM12S (48.5 mpH/min) cells suggesting that all cell lines responded by increasing metabolic activity (Figure 7A). Comparison of oxygen consumption rates (OCR) basal metabolism was determined for MLC (164.2 pmol/min), HB-EGF (99.3 pmol/min), ADAM12S (190.67 pmol/min), and HB-EGF/ADAM12S (177.5 pmol/min). No differences were observed for the basal conditions other than HB-EGF OCR being significantly lower (Figure 7B). Basal rates were compared when exposed to catecholamines for oxygen consumption and HB-EGF/ADAM12S (222.2 pmol/min) was significantly

increased while MLC (194.7 pmol/min), HB-EGF (108.2 pmol/min), and ADAM12S (177.5 pmol/min) were not. Upon exposure of cells lines to FCCP+Oligomycin, MLCs (337.8 pmol/min), HB-EGF (194.2 pmol/min), ADAM12S (286.1 pmol/min), and HB-EGF/ADAM12S (447.9 pmol/min) were increased compared to their basal rates (Figure 7). Basal ratios of OCR:ECAR were determined for MLC (8.3), HB-EGF (7.2), ADAM12S (10.5), and HB-EGF/ADAM12S (10.6). No significant differences in the ratios when exposed to catecholamines for MLC (9.4), ADAM12 (8.7), and HB-EGF/ADAM12S (12.5) were observed; however, HB-EGF (11.8) exhibited an increased (Figure 8A). When exposed to FCCP+Oligomycin, MLC (7.3) and HB-EGF (7.0) demonstrated no difference when compared to basal rates while ADAM12S (6.4) and HB-EGF/ADAM12S (8.7) demonstrated a decrease. All samples were then analyzed for their % change (Table 1).

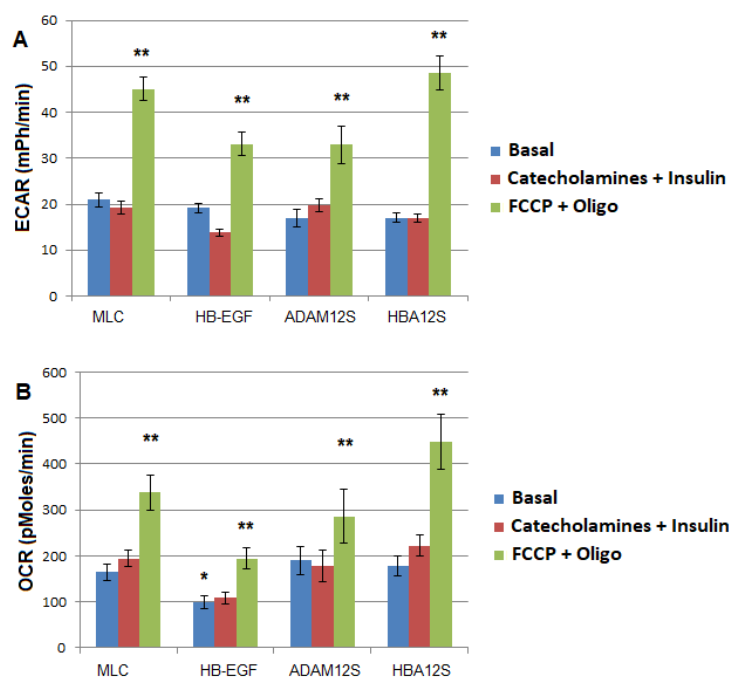


**Figure 7.** Metabolic output of HB-EGF/ADAM 12S co-expressing cells. Metabolic parameters of MLCs (n = 4), HB-EGF (n = 3), ADAM 12S (n = 3), and HB-EGF/ADAM 12S co-expressing cells (n = 4) was measured using Seahorse XF24 at basal, after catecholamine exposure, and then when stressed with FCCP+Oligomycin exposure. Extracellular acidification rate (ECAR) was used to determine the amount of glycolysis (panel A). Oxygen consumption rate (OCR) was measured to determine the amount of oxidative phosphorylation (panel B). \* compares cell's basal rate to MLC basal rate. \*\* compares treatment of cell type to basal of same cell type. ( $p$ -value < 0.05).

These results suggest that HB-EGF/ADAM12S cells are activated by catecholamines and the fuel source for oxidative phosphorylation appears to be from more than glycolysis alone. However, for this to be relevant for obesity studies, the HB-EGF/ADAM 12S co-expressing cells were compared to BAT. In order to compare these cells to BAT, 3T3-L1 cells were differentiated into BAT, as described above. Basal rates for ECAR were determined for 3T3-L1 (8.1 mpH/min), WAT (9.2 mpH/min), HB-EGF/ADAM12S (28.3 mpH/min) and BAT (20.4 mpH/min) (Figure 9A) and all were significantly increased compared to 3T3-L1 cells. When comparing catecholamine exposure to basal conditions there

was no change in any of the cell lines. Comparison of FCCP+Oligomycin exposure to basal conditions, 3T3-L1 (19.1 mpH/min), WAT (25.1 mpH/min), HB-EGF/ADAM12S (110.9 mpH/min) and BAT (55.3 mpH/min) demonstrated a significant increase. Oxygen consumption basal rates for 3T3-L1 (12.6 pmol/min), WAT (40.5 pmol/min), HB-EGF/ADAM12S (297.2 pmol/min), and BAT (155.1 pmol/min) were determined (Figure 9B). Comparing catecholamine exposure to basal conditions results in increases for 3T3-L1 (43.9 pmol/min), WAT (81.7 pmol/min), HB-EGF/ADAM12S (398.3 pmol/min), and BAT (252.8 pmol/min). Comparison of FCCP+Oligomycin exposure to basal conditions, 3T3-L1 (59.8 pmol/min), WAT (128.4 pmol/min), HB-EGF/ADAM12S (672.5 pmol/min), and BAT (473.3 pmol/min) are all increased. OCR:ECAR basal rates were established for 3T3-L1 (1.6), WAT (5.1), HB-EGF/ADAM12S (10.8) and BAT (10.3), where WAT, HB-EGF/ADAM12S, and BAT are all significantly increased compared to 3T3-L1 cells (Figure 8B). Comparing ratios once exposed to catecholamines to basal ratios results in 3T3-L1 (5.8) and WAT (9.7) being significantly increased while HB-EGF/ADAM12S (12.3) and BAT (11.1) were not. Comparing FCCP+Oligomycin to basal ratios, 3T3-L1 (3.14) was significantly increased, WAT (5.1) and BAT (8.9) resulted in no change, and HB-EGF/ADAM12S (5.8) was significantly decreased. All samples were then analyzed for their % change (Table 2).

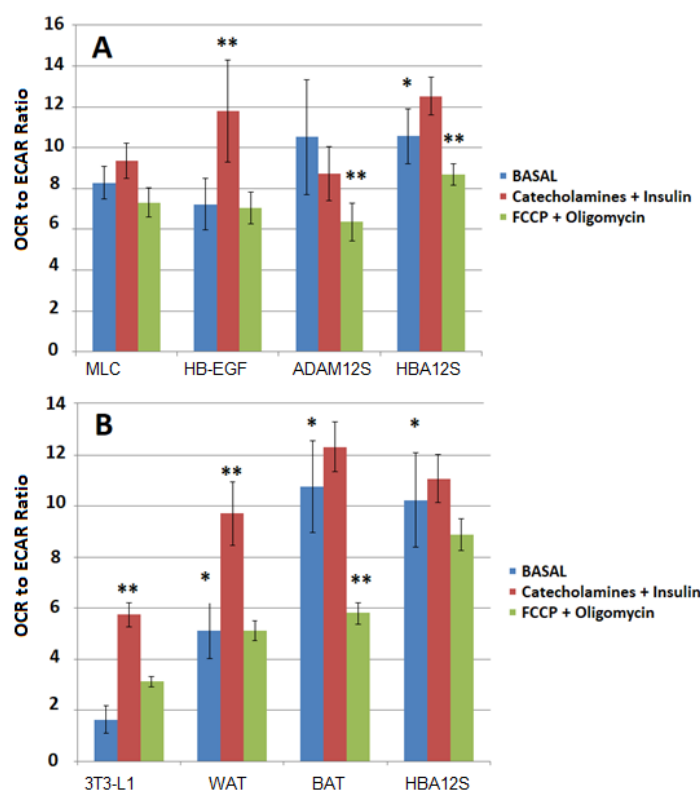


**Figure 8.** Ratio of Oxygen Consumption to Glycolysis in HB-EGF/ADAM 12S co-expressing cells. The OCR: ECAR ratio for MLC (n = 4), HB-EGF (n = 3), ADAM 12S(n = 3), and HB-EGF/ADAM 12S cells (n = 4) under basal, catecholamine + insulin, and once stressed with FCCP+Oligomycin (Panel A). The OCR:ECAR ratio for 3T3-L1 (n = 5), WAT (n = 5), HB-EGF/ADAM 12S cells (n = 5), and BAT (n = 5) under basal, catecholamine + insulin, and once stressed with FCCP+Oligomycin (Panel B). \* compares cell's basal rate to MLC basal rate. \*\* compares treatment of cell type to basal of same cell type. ( $p$ -value < 0.05).

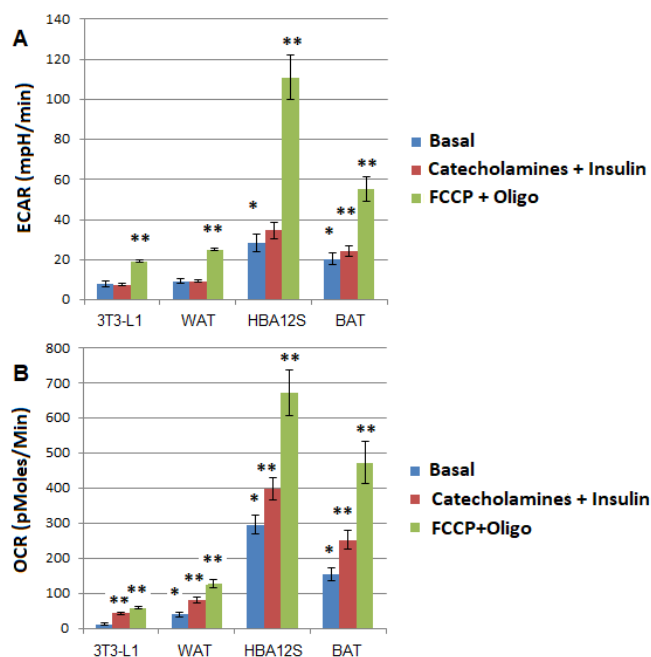


**Figure 9.** Metabolic output of HB-EGF/ADAM 12S co-expressing cells compared to WAT and BAT. Metabolic parameters of 3T3-L1 ( $n = 5$ ), WAT induced 3T3-L1 cells ( $n = 5$ ), BAT induced 3T3-L1 cells ( $n = 5$ ), and HB-EGF/ADAM 12S co-expressing cells ( $n = 5$ ) were measured using a Seahorse XF 24 (Agilent) at basal, after catecholamine exposure, and when stressed with FCCP+Oligomycin exposure. Extracellular acidification rate (ECAR) was used to determine the amount of glycolysis (panel A). Oxygen consumption rate (OCR) was measured to determine the amount of oxidative phosphorylation (panel B). \* compares cells basal rate to 3T3 basal rate. \*\* compares treatment of cell type to basal of same cell type. ( $p$ -value  $< 0.05$ ).

**Table 1.** Metabolic potential of HB-EGF/ADAM 12S cells compared to mouse fibroblasts. %change from basal for MLC, MLC + HB-EGF, MLC + ADAM 12S, and HB-EGF/ADAM 12S cells when exposed to catecholamines and insulin or FCCP+Oligomycin for both ECAR and OCR as measured on Seahorse XF 24.

Treatment Type	Cell Type	%Change ECAR	%Change OCR
Catecholamines + Insulin	MLC	-7.8	18.6
	ADAM 12S	16.5	-6.9
	HB-EGF	-28.1	9.0
	HB-EGF/ADAM 12S	-0.3	25.2
FCCP + Oligomycin	MLC	115.7	105.8
	ADAM 12S	93.5	50.0
	HB-EGF	72.7	95.5
	HB-EGF/ADAM 12S	184.6	152.4

**Table 2.** Metabolic potential of HB-EGF/ADAM 12S cells compared to other adipocytes. %change from basal for 3T3-L1, WAT induced 3T3-L1 cells, BAT induced 3T3-L1 cells, and HB-EGF/ADAM 12S cells when exposed to catecholamines and insulin or FCCP + Oligomycin for both ECAR and OCR as measured on a Seahorse XF 24.

Treatment Type	Cell Type	%Change ECAR	%Change OCR
Catecholamines + Insulin			
	3T3-L1	-7.8	248.2
	WAT	-0.8	101.5
	BAT	19.6	63.0
	HB-EGF/ADAM 12S	22.6	34.0
FCCP + Oligomycin			
	3T3-L1	136.2	374.6
	WAT	172.5	216.7
	BAT	170.9	205.2
	HB-EGF/ADAM 12S	291.6	126.3

#### 4. Discussion

BAT is a known metabolic tissue that dissipates energy as heat under cold conditions and adrenergic stimulation [19]. Co-expression of HB-EGF and ADAM12S in MLCs and human epidermoid carcinoma (A431) cells results in multilocular lipid accumulation, increased mitochondrial staining, and changes in mRNA expression to a more BAT-like phenotype thus suggesting that these cells reprogrammed into BAT [7,8].

The increased expression of FGF2, KLF3, and PGC-1 $\alpha$ , and decreased expression of CEBP $\alpha$  and GLUT4 in HB-EGF/ADAM 12S co-expressing cells has been previously identified as key components in BAT cellular reprogramming [8]. FGF2 maintains induced pluripotent stem-cells [20]. KLF3 is important for adipogenesis to occur as KLF3 knockout mice are lean and protected against diet induced obesity [21]. Interestingly, KLF3 is a repressor of C/EBP $\alpha$  [22] and C/EBP $\alpha$  is required for WAT differentiation but not BAT [23], thus KLF3 regulates adipocyte differentiation. PGC-1 $\alpha$  regulates mitochondrial biogenesis and is highly expressed in BAT but not WAT [19]. GLUT4 is highly expressed in WAT and BAT but low levels of GLUT4 is an indicator of immature BAT [24]. This evidence suggests that HB-EGF/ADAM 12S co-expression directs cellular reprogramming into BAT and not WAT. WAT differentiation is likely prevented by increased expression of KLF3 and decreased expression of C/EBP $\alpha$ . Additionally, the HB-EGF/ADAM 12S co-expressing cells are more metabolically active, likely due to increased expression of PGC-1 $\alpha$  that results in enhanced mitochondrial staining [7].

To further support the hypothesis that HB-EGF/ADAM 12S co-expressing cells direct BAT cellular reprogramming, a stem-cell transcription factor microarray was employed. The array exhibited up-regulation of two HOX genes, C5 and A10. HOX genes are known to be involved in determining segment identity during development [25]. HOXC5 has been implicated in intramuscular fat accumulation [26] and supports results in which transgenic mice that direct ADAM 12S muscle specific expression exhibit increased intramuscular fat accumulation [27]. Increased HOXA10 gene expression occurs via *in vitro* culturing of brown fat stromal vascular fraction cells when exposed to differentiation inducing agents such as IBMX [28]. The increased expression of HOXA10 and HOXC5

further supports a cellular reprogramming hypothesis in HB-EGF/ADAM 12S BAT-like cells.

In order to determine the metabolic potential of HB-EGF/ADAM 12S co-expressing cells, oxygen consumption and extracellular acidification rates were examined. HB-EGF ADAM12S co-expressing cells exhibited increased oxygen consumption rates (OCR) that reflects 3T3-L1 induced BAT-like cells. Furthermore, exposure of HB-EGF/ADAM 12S co-expressing cells and 3T3-L1 induced BAT-like cells to catecholamines increased OCR by 19.8% and 62.8 %, respectively. Whereas, 3T3-L1 WAT-like cells and 3T3-L1 cells increased by 576.2% and 180% respectively and exhibited low basal levels of OCR even after being exposed to catecholamines or FCCP+Oligomycin. They failed to reach the same level of metabolic activity as HB-EGF/ADAM12S and BAT reached at basal levels. The 62.8% increase in OCR of 3T3-L1 catecholamine induced BAT is similar to previous studies [29] in which 3T3-L1 BAT catecholamine exposure resulted in a 70% increase in OCR, while UCP-1 silenced cells exhibited an increase of 30%. The lower % change in HB-EGF/ADAM12S may indicate that these cells are not fully mature or it could just be a result of having a much higher basal metabolic rate.

Glucose utilization in BAT is important for metabolic activity and lipid accumulation; however, upon adrenergic stimulation or cold exposure, lipolysis occurs as a result of increased use of lipids as a fuel source for non-shivering thermogenesis. Interestingly, UCP-2 knockout mice demonstrate increased glucose uptake and utilization under stress conditions, but reduced thermogenic activity due to impairment in oxidative uncoupling and a preference for glucose utilization [30]. In contrast, UCP-2 expression results in fatty acid oxidation and limits pyruvate utilization from glycolysis [31,32]. 3T3-L1 BAT-like cells demonstrated an increase in glucose utilization but HB-EGF/ADAM12S co-transfected MLCs lacked an increase in glucose utilization. However, both 3T3-L1 and HB-EGF/ADAM 12S co-expressing cells exhibited a positive % change while 3T3-L1 and 3T3-L1 induced WAT-like cells exhibited a negative % change. Collectively, these findings suggest that HB-EGF/ADAM12S co-expressing BAT-like reprogrammed cells are more metabolically active than controls cells and may have a preference for fatty acid oxidation rather than glucose utilization and provides further support that HB-EGF/ADAM 12S cellular reprogramming into BAT-like cells may be powerful therapeutic tool to combat obesity.

To better determine whether HB-EGF/ADAM12S co-expressing cells and 3T3-L1 BAT-like cells are similar the OCR:ECAR (oxygen consumption rate: glucose utilization rate) ratios were examined. HB-EGF/ADAM12S co-transfected MLCs and 3T3-L1 induced BAT-like cells are more metabolically active during basal conditions for both oxygen consumption and glycolysis but the ratio is highly tilted towards oxygen consumption (10.78, 10.26) when compared to 3T3-L1 and 3T3-L1 WAT-like cells (1.63, 5.12). When activated by catecholamines, 3T3-L1 cells and 3T3-L1 induced WAT-like cells ratio increased by 482% and 97% percent, respectively, while HB-EGF/ADAM12S co-transfected BAT-like cells and 3T3-L1 induced BAT-like cells increased by 7% and 8%, respectively. These results could suggest that acetyl-CoA is provided not only by glycolysis, but also by other carbon sources, such as  $\beta$ -oxidation of fats, utilized by HB-EGF/ADAM12S and 3T3-L1 BAT-like cells for metabolism.

HB-EGF/ADAM12S co-expressing cells demonstrate a change in OCR:ECAR ratio when exposed to FCCP+Oligomycin stressors. Oligomycin binds to ATP synthase and prevents protons from reentering the mitochondria, disrupting the gradient and stopping the proton pump from functioning [33]. As a result, the cell will increase glycolysis in an attempt to regain the lost ATP. FCCP disrupts the membrane potential of the mitochondria resulting in depolarization of the membrane, causing oxidative

phosphorylation to increase in an attempt to re-polarize the membrane [34–38]. The stressor mix resulted in increases in OCR and ECAR in all cell types. OCR increases in BAT when exposed to FCCP is well documented [39–41]. Oligomycin dissipates ATP more effectively in BAT than in liver [42]. This increased ability to disrupt ATP synthase is believed to be a result of BAT's ability to uncouple oxidative phosphorylation from ATP synthesis. HB-EGF/ADAM12S cells demonstrate an increase in OCR and ECAR suggesting that both oligomycin and FCCP are effectively stressing these cells. This stressor combination causes HB-EGF/ADAM12S cells' OCR:ECAR ratio to drop significantly below basal levels while WAT and 3T3-L1 cells ratios remain unchanged and are similar to their basal levels. These results suggest that glycolysis is now providing HB-EGF/ADAM12S cells more acetyl-CoA while under stressed conditions than under basal or catecholamine exposure conditions.

PGC-1 $\alpha$  expression levels are increased in HB-EGF/ADAM12S co-expressing cells [7,8] which supports the increased metabolic data in these cells. PGC-1s are important for lipid metabolism as demonstrated by  $\beta$ -cells that have reduced levels of PGC-1s and exhibit increased accumulation of acyl-glycerols, while  $\beta$ -cells without reduced PGC-1s do not accumulate acyl-glycerols [43]. Previous results have demonstrated that KLF4 is up-regulated in HB-EGF/ADAM12S co-expressing cells [8]. Interestingly, UCP-1 knockout mice exhibit lower oxygen consumption rates than their wild type counterparts [44]. UCP-1 expression levels are up-regulated in HB-EGF/ADAM12S cells [7] which further supports the increased metabolic results of HB-EGF/ADAM 12S reprogrammed BAT cells.

In summary, HB-EGF and ADAM12S co-expression stimulates cellular reprogramming into BAT-like cells that, in part, requires the up-regulation of PGC-1 $\alpha$ , Klf3, FGF2, down-regulation of C/EBP- $\alpha$  proteins, and up-regulation of HOXA10 and HOXC5 mRNA. Furthermore, HB-EGF/ADAM 12S reprogrammed cells exhibit similar characteristics to metabolically active BAT, responds to catecholamine exposure similar to BAT, and provides supportive evidence for HB-EGF and ADAM 12S as therapeutic tools to combat obesity.

## Acknowledgements

We would like to Acknowledge Dr. Zaza Khuchua and Caitlin Schafer from Cincinnati Children's Hospital for their help on the seahorse experiments.

## Conflict of Interest

All authors declare no conflicts of interest.

## References

1. Giordano A, Smorlesi A, Frontini A, et al. (2014) White, brown and pink adipocytes: the extraordinary plasticity of the adipose organ. *Eur J Endocrinol* 170: R159–171.
2. Bateurs D, Cobbaut M, Geys L, et al. (2017) Loss of ADAMTS5 enhances brown adipose tissue mass and promotes browning of white adipose tissue via CREB signaling. *Mol Metab* 6: 715–724.
3. Cristancho AG, Lazar MA (2011) Forming functional fat: a growing understanding of adipocyte differentiation. *Nat Rev Mol Cell Biol* 12: 722–734.
4. Porter RK (2006) A new look at UCP 1. *Biochim Biophys Acta* 1757: 446–448.

5. Nedergaard J, Golozoubova V, Matthias A, et al. (2001) UCP1: the only protein able to mediate adaptive non-shivering thermogenesis and metabolic inefficiency. *Biochim Biophys Acta* 1504: 82–106.
6. Ghorbani M, Himms-Hagen J (1997) Appearance of brown adipocytes in white adipose tissue during CL 316,243-induced reversal of obesity and diabetes in Zucker fa/fa rats. *Int J Obes Relat Metab Disord* 21: 465–475.
7. Zhou Z, Darwal MA, Cheng EA, et al. (2013) Cellular reprogramming into a brown adipose tissue-like phenotype by co-expression of HB-EGF and ADAM 12S. *Growth Factors* 31: 185–198.
8. Taylor SR, Klements JR, Markesbery MG, et al. (2014) Cellular transdifferentiation into brown adipose-like cells by adenoviral-directed expression or stable transfection of HB-EGF and ADAM 12S. *J Cell Mol Biol* 12: 55–62.
9. Christiaens V, Scroyen I, Lijnen HR (2008) Role of proteolysis in development of murine adipose tissue. *Thromb Haemost* 99: 290–294.
10. Sun K, Kusminski CM, Scherer PE (2011) Adipose tissue remodeling and obesity. *J Clin Invest* 121: 2094–2101.
11. Odaka M, Kohda D, Lax I, et al. (1997) Ligand-binding enhances the affinity of dimerization of the extracellular domain of the epidermal growth factor receptor. *J Biochem* 122: 116–121.
12. Suzuki M, Raab G, Moses MA, et al. (1997) Matrix metalloproteinase-3 releases active heparin-binding epidermal growth factor by cleavage at a specific juxtamembrane site. *J Biol Chem* 272: 31730–31737.
13. Asakura M, Kitakaze M, Takashima S, et al. (2002) Cardiac hyper-trophy is inhibited by antagonism of ADAM12 processing of HB-EGF: metalloproteinase inhibitors as a new therapy. *Nat Med* 8: 35–40.
14. Nanba D, Mammoto A, Hashimoto K, et al. (2003) Proteolytic release of the carboxy-terminal fragment of pro-HB-EGF causes nuclear export of PLZF. *J Cell Biol* 163: 489–502.
15. Higashiyama S, Nanba D (2005) ADAM-mediated ectodomain shedding of HB-EGF in receptor cross-talk. *Biochim Biophys Acta* 1751: 110–117.
16. Kurisaki T, Masuda A, Sudo K, et al. (2003) Phenotypic analysis of Meltrin alpha (ADAM12)-deficient mice: involvement of Meltrin alpha in adipogenesis and myogenesis. *Mol Cell Biol* 23: 55–61.
17. Taylor SR, Markesbery MG, Harding PA (2014) Heparin-binding epidermal growth factor-like growth factor (HB-EGF) and proteolytic processing by a disintegrin and metalloproteinases (ADAMs): a regulator of several pathways. *Semin Cell Dev Biol* 28: 22–30.
18. Asano H, Kanamori Y, Higurashi S, et al. (2014) Induction of beige-like adipocytes in 3T3-L1 cells. *J Vet Med Sci* 76: 57–64.
19. Lowell BB, Spiegelman BM (2000) Towards a molecular understanding of adaptive thermogenesis. *Nat* 404: 652–660.
20. Vallier L, Touboul T, Brown S, et al. (2009) Signaling pathways controlling pluripotency and early cell fate decisions of human induced pluripotent stem cells. *Stem Cells* 27: 2655–2666.
21. Bell-Anderson KS, Funnell AP, Williams H, et al. (2013) Loss of Krüppel-like factor 3 (KLF3/BKLF) leads to upregulation of the insulin-sensitizing factor adipolin (FAM132A/CTRP12/C1qdc2). *Diabetes* 62: 2728–2737.
22. Sue N, Jack BH, Eaton SA, et al. (2008) Targeted disruption of the basic Krüppel-like Factor Gene (Klf3) reveals a role in adipogenesis. *Mol Cell Bio* 28: 3967–3978.

23. Linhart HG, Ishimura-Oka K, DeMayo F, et al. (2001) C/EBP alpha is required for differentiation of white, but not brown, adipose tissue. *Proc Natl Acad Sci U S A* 98: 12532–12537.
24. Shimizu Y, Shimazu T (2002) Thyroid hormone augments GLUT4 expression and insulin-sensitive glucose transport system in differentiating rat brown adipocytes in culture. *J Vet Med Sci* 64:677–681.
25. Myers P (2008) Hox genes in development: The Hox code. *Nat Education* 1: 1–4.
26. Cesar AS, Regitano LC, Koltjes JE, et al. (2015) Putative regulatory factors associated with intramuscular fat content. *PLoS One* 10: e0128350.
27. Kawaguchi N, Xu X, Tajima R, et al. (2002) ADAM 12 protease induces adipogenesis in transgenic mice. *Am J Pathol* 160: 1895–1903.
28. Singh S, Rajput YS, Barui AK, et al. (2016) Fat accumulation in differentiated brown adipocytes is linked with expression of Hox genes. *Gene Expr Patterns* 20: 99–105.
29. Isidor MS, Winther S, Basse AL, et al. (2015) An siRNA-based method for efficient silencing of gene expression in mature brown adipocytes. *Adipocyte* 5: 175–185.
30. Caron A, Labbé SM, Carter S, et al. (2017) Loss of UCP2 impairs cold-induced non-shivering thermogenesis by promoting a shift toward glucose utilization in brown adipose tissue. *Biochimie* 134: 118–126.
31. Pecqueur C, Bui T, Gelly C, et al. (2008) Uncoupling protein-2 controls proliferation by promoting fatty acid oxidation and limiting glycolysis-derived pyruvate utilization. *FASEB J* 22: 9–18.
32. Pecqueur C, Alves-Guerra C, Ricquier D, et al. (2009) UCP2, a metabolic sensor coupling glucose oxidation to mitochondrial metabolism? *IUBMB Life* 61:762–767.
33. Lee O, O'Brien PJ (2010) 1.19-Modifications of mitochondrial function by toxicants. *Compr Toxicol* 1:411–445.
34. Heytler PG, Prichard WW (1962) A new class of uncoupling agents—carbonyl cyanide phenylhydrazones. *Biochem Biophys Res Commun* 7: 272–275.
35. Hyllienmark L, Brismar T (1996) Effect of metabolic inhibition on K<sup>+</sup> channels in pyramidal cells of the hippocampal CA1 region in rat brain slices. *J Physiol* 496: 155–164.
36. Buckler KJ, Vaughan-Jones RD (1998) Effects of mitochondrial uncouplers on intracellular calcium, pH and membrane potential in rat carotid body type I cells. *J Physiol* 513:819–833.
37. Park KS, Jo I, Pak K, et al. (2002) FCCP depolarizes plasma membrane potential by activating proton and Na<sup>+</sup> currents in bovine aortic endothelial cells. *Pflügers Arch* 443: 344–352.
38. To MS, Aromataris EC, Castro J, et al. (2010) Mitochondrial uncoupler FCCP activates proton conductance but does not block store-operated Ca<sup>2+</sup> current in liver cells. *Arch Biochem Biophys* 495: 152–158.
39. Prusiner SB, Cannon B, Ching TM et al. (1968) Oxidative metabolism in cells isolated from brown adipose tissue. 2. Catecholamine regulated respiratory control. *Eur J Biochem* 7: 51–57.
40. Reed N, Fain JN (1968) Stimulation of respiration in brown fat cells by epinephrine, dibutyryl-3',5'-adenosine monophosphate, and m-chloro (carbonyl cyanide) phenylhydrazone. *J Biol Chem* 243: 2843–2848.
41. Mohell N, Connolly E, Nedergaard J (1987) Distinction between mechanisms underlying alpha 1- and beta-adrenergic respiratory stimulation in brown fat cells. *Am J Physiol* 253:C301–308.
42. Flatmark T, Pedersen JI (1973) Studies on the energy state of isolated brown adipose tissue mitochondria. Effect of adenine nucleotides and oligomycin on the generation and dissipation of the "energy potential". *Biochim Biophys Acta* 292: 64–72.

43. Oropeza D, Jouvét N, Bouyakdan K, et al. (2015) PGC-1 coactivators in  $\beta$ -cells regulate lipid metabolism and are essential for insulin secretion coupled to fatty acids. *Mol Metab* 4: 811–822.
44. Dlasková A, Clarke KJ, Porter RK (2010) The role of UCP 1 in production of reactive oxygen species by mitochondria isolated from brown adipose tissue. *Biochim Biophys Acta* 1797: 1470–1476.



AIMS Press

© 2018 the Author(s), licensee AIMS Press. This is an open access article distributed under the terms of the Creative Commons Attribution License (<http://creativecommons.org/licenses/by/4.0>)